A&A 475, 479–485 (2007)
DOI: 10.1051/0004-6361:20077366

Astronomy & Astrophysics

Luminous HC_3N line and the HCN/HCO^+ ratio in NGC 4418

Buried AGN or nascent starburst?

S. Aalto[1], R. Monje[1], and S. Martín[2]

[1] Onsala Space Observatory, S-439 94 Onsala, Sweden
e-mail: [susanne;raquel]@oso.chalmers.se
[2] Harvard-Smithsonian Center for Astrophysics, 60 Garden Street, Cambridge, MA 02138, USA

Received 27 February 2007 / Accepted 27 June 2007

ABSTRACT

Aims. We investigate the properties of the nuclear molecular gas and address the nature of the deeply buried source driving the IR emission of NGC 4418.
Methods. We present IRAM 30 m observations and basic non-LTE, single component radiative transport modelling of HNC, HCN, HCO^+, CN, HC_3N, and H_2CO
Results. We find that NGC 4418 has a rich molecular chemistry – including unusually luminous HC_3N J = 10–9, 16–15, and 25–24 line emission – compared to the other high density tracers. We furthermore detect: ortho-H_2CO 2–1, 3–2; CN 1–0, 2–1; HCO^+, 1–0. 3–2, HCN 3–2, HNC 1–0, 3–2, and tentatively OCS 12–11. The HCN, HCO^+, H_2CO, and CN line emission can be fitted to densities of $n = 5\times10^4$–10^5 cm^{-3} and gas temperatures T_k = 80–150 K. Both HNC and HC_3N are, however, significantly more excited than the other species, which requires higher gas densities or radiative excitation through mid-IR pumping. The HCN line intensity is fainter than that of HCO^+ and HNC for the 3–2 transition, in contrast to previous findings for the 1–0 lines, where the HCN emission is the most luminous. Assuming all line emission is emerging from the same gas, abundances of the observed species are estimated to be similar to each other within factors of 2–5. The most noteworthy of these is the high abundance of HC_3N and a small-to-moderate abundance ratio between HCN and HCO^+.
Conclusions. We tentatively suggest that the observed molecular line emission is consistent with a young starburst, where the emission can be understood as emerging from dense, warm gas with an additional PDR component. We find that X-ray chemistry is not required to explain the observed mm-line emission, including the HCN/HCO^+ 1–0 and 3–2 line ratios. The luminous HC_3N line emission is an expected signature of dense, starforming gas. A deeply buried AGN cannot be excluded, but its impact on the surrounding molecular medium is then suggested to be limited. However, detailed modelling of HC_3N abundances in X-ray dominated regions (XDRs) should be carried out. The possibility of radiative excitation should also be investigated further.

Key words. galaxies: evolution – galaxies: individual: NGC 4418 – galaxies: starburst – galaxies: active – radio lines: ISM – ISM: molecules

1. Introduction

Since their discovery by the Infrared Astronomical Satellite (IRAS), luminous infrared galaxies (LIRGs, $L_{IR} > 10^{11}\ L_\odot$) have been studied at almost all wavelengths (e.g. Sanders & Mirabel 1996). They radiate most of their luminosity as dust thermal emission in the infrared. However, the nature of the main power source (a starburst, an active galactic nucleus (AGN), or a combination of both) is still unclear.

NGC 4418 is a nearly edge-on Sa-type galaxy with deep mid-infrared silicate absorption features, suggesting that the inner region is enshrouded by large masses of warm (85 K) dust (e.g. Spoon et al. 2001; Evans et al. 2003). Due to the high obscuration, it is difficult to determine the nature of the activity that is driving the luminosity. The infrared luminosity to molecular gas mass ratio – $L_{IR}/M(H_2)$ = 100 is high for a non-ULIRG galaxy (Sanders et al. 1991). Furthermore, NGC 4418 has a high infrared to radio continuum ratio $q \approx 3$ (q = the logarithmic ratio of far-infrared (FIR) to radio flux densities). This FIR-excess may be caused by a young, somewhat synchrotron-deficient, starburst (Roussel et al. 2003). The lack of hard X-ray emission (Cagnoni et al. 1998) and a resolved radio continuum emission support the starburst interpretation.

In contrast, Seyfert-like infrared colours indicate that the dust in NGC 4418 is being heated by an obscured AGN. Imanishi et al. (2004) find broad NIR H_2 lines and a mm HCN/HCO^+ J = 1–0 line ratio of >1 – which, they suggest, support the notion of an obscured AGN. The lack of hard X-rays may in this context be due to the AGN being Compton thick.

The molecular line ratio HCN/HCO^+ 1–0 has been suggested as a diagnostic tool for identifying the effect of an AGN on its surrounding molecular ISM (e.g. Kohno et al. 2001; Imanishi et al. 2004). The X-rays from the AGN impact the interstellar medium (ISM) surrounding it, creating an XDR – an X-ray dominated region. Since X-rays may penetrate deep into the surrounding ISM, the resulting XDR may become large and affect molecular properties on large scales. Molecular line ratios are therefore potentially useful as XDR indicators. According to models by e.g. Maloney et al. (1996), HCO^+ is destroyed in XDRs, while HCN may enjoy high abundances, resulting in an elevated HCN/HCO^+ 1–0 line ratio. Recent XDR models, however, question the suggested underabundance of HCO^+ in XDRs (e.g. Meijerink & Spaans 2005; Meijerink et al. 2006, 2007) and find HCN and HCO^+ abundances to be similar – or HCO^+ to be somewhat overabundant. Thus, the interpretation of an elevated HCN/HCO^+ 1–0 line ratio is not straightforward,

Table 1. Observational parameters and Gaussian line fits.

Line	ν^a [GHz]	HPBW^b [″]	$\eta_{mb}{}^c$	$I^d = \int T_A^* dV$ [K km s^{-1}]	$V_c{}^e$ [km s^{-1}]	ΔV^f [km s^{-1}]	T_A^{*h} [mK]
CO 1–0	115.271	21	0.74	14.6 ± 0.7	2110	120	114.0
CO 2–1	230.538	10	0.53	20.2 ± 0.9	2114	107	157.0
CN 1–0	113.491	22	0.74	1.50 ± 0.25	2081	154	8.5
CN 2–1^i	226.875	11	0.53	2.46 ± 0.2^j	2115	150	7.8
CN 2–1^k	226.659	11	0.53	...	...	215	5.5
HCO^+ 1–0	89.188	28	0.77	1.74 ± 0.12	2110	150	9.9
HCO^+ 3–2	267.558	9.2	0.45	4.1 ± 0.6	2120	190	21.5
HCN 3–2	265.886	9.4	0.46	2.4 ± 0.3	2110	240	9.3
HNC 1–0	90.664	27	0.77	1.24 ± 0.12	2120	156	7.5
HNC 3–2	271.981	9	0.44	4.97 ± 0.6	2120	150	29.3
HC_3N 10–9	90.979	27	0.77	0.8 ± 0.08	2110	122	6.4
HC_3N 16–15^l	145.561	17	0.70	1.7 ± 0.08	2120	130	8.6
HC_3N 25–24	227.419	11	0.53	1.6 ± 0.2	2130	140	10.0
HNCO 4–3	87.925	28	0.77	<0.36 (3σ)	...	...	...
H_2CO 2–1	140.839	17	0.70	1.05 ± 0.2	2156	145	5.7
H_2CO 3–2	225.698	11	0.53	0.6 ± 0.3	2140	145	3.6
OCS 12–11	145.947	17	0.70	0.8 ± 0.14	...	174	4.8

[a] Rest frequency. [b] Beam width. [c] Main beam efficiency. [d] Integrated intensity. in T_A^*, uncorrected for beam efficiency and beam size. [e] Centre velocity of the line. [f] Line width from Gaussian fit. [h] Peak intensity from Gaussian fit. [i] First spingroup. [j] Including both first and second spingroup. [k] Second spingroup. [l] HC_3N 16–15 is contaminated by para-H_2CO. Its contribution is estimated to 20%. Fitted Gaussians and integrated intensities are only for the HC_3N component (see text).

in particular when line opacities and excitation are taken into account. Furthermore, dense gas with low ionization levels may also have a relative underabundance of HCO^+. Therefore, further observations and modelling is necessary for assessing the impact of AGNs and starbursts on their surrounding ISM.

We carried out an initial molecular line search of NGC 4418 with the IRAM 30 telescope. The goal was to observe multiple transitions of high-density tracer molecules and to search for complex molecules to get a first handle on the molecular ISM conditions of NGC 4418. High-density tracer molecules require gas densities in excess of 10^4 cm^{-3} in order to be collisionally excited. This is two orders of magnitude greater than the ^{12}CO 1–0 line, which is the most commonly used tracer of molecular gas in external galaxies.

We find a surprisingly rich ISM chemistry in NGC 4418 with very luminous HC_3N line emission, and that the HCN 3–2 line emission is fainter than both HCO^+ and HNC 3–2. In Sect. 2, observations and results in terms of line intensities, ratios, and RADEX models are presented. In Sect. 3, we discuss the interpretation of the luminous HC_3N line and the other line intensities in the context of XDR and starburst scenarios. We tentatively suggest a starburst scenario and briefly present how this conclusion may be tested.

2. Observations and results

We have used the IRAM 30 m telescope to observe 1 mm, 2 mm and 3 mm lines of HNC, HCO^+, HCN, CN, HC_3N, Ortho-H_2CO, CO, and HNCO towards the centre of the luminous galaxy NGC 4418. Observations were made in May and July 2006, and the system noise temperatures were typically 150 K and 500 K for the 3 mm and 1 mm lines, respectively. Pointing was checked regularly on nearby continuum sources and rms was found to vary between 1.5″ and 2″. Beamsizes and efficiencies are shown in Table 1. Intensities are presented in T_A^* scale. T_A^* is transferred into the main beam brightness scale, T_{mb}, through dividing T_A^* by the beam efficiency η_{mb} and multiplying by the forward efficiency, η_f. Values for η_f are 0.95 (3 mm), 0.93 (2 mm), 0.91 (1.3 mm) and 0.88 (1 mm).

First-order baselines have been removed from all spectra. Weather conditions during both runs were close to normal summer conditions with precipitable water vapour: pwv = 4.3–5.1 mm in May and pwv = 3.5–4.1 mm in June. The 1 mm observations of HCN and HNC 3–2 were repeated in the July run to confirm the line ratios. We found that line intensities could be repeated within 15% suggesting that, in general, 1 mm conditions in both May and July were stable. We also repeated the H_2CO 2–1 2 mm line and found that the line intensity was repeatable within 10%.

2.1. Line intensities and ratios

We have detected the following line emission: HNC 1–0, 3–2; HCO^+ 1–0, 3–2; HCN 3–2, CN 1–0, 2–1; HC_3N 10–9, 16–15, 25–24; Ortho-H_2CO 2–1 and 3–2; CO 1–0, 2–1 (see Fig. 1, Table 1). We also tentatively detect the OCS 12–11 line at the edge of the HC_3N 16–15 band. HNCO 4–3 was not detected down to an rms level of 2 mK. In Fig. 1 we have marked the position of the HC_3N J = 10–9, v_6 = 1–0 rotational-vibrational transition, and the CH_3OH 3–2 line. They are both 2σ detections if one only considers the rms. More observations are required to confirm their presence. Integrated line intensities and fitted Gaussian line parameters are presented in Table 1. A para-H_2CO 2–1 line is blended with the HC_3N 16–15 line (para-H_2CO is shifted +42 MHz or −82 km s^{-1} from the HC_3N line). A Gaussian fit where we set the velocity of the line centre to 2120 km s^{-1} and the line width to 130 km s^{-1} result in an estimate of the para-H_2CO contribution to 20% of the total integrated line intensity. This implies an H_2CO 2–1 ortho/para line ratio of >2 (see Table 1 for the Ortho 2–1 line intensity). In warm gas ($T_k \gtrsim 40$ K) the ortho-to-para ratio is close to the statistical ratio of 3 (e.g. Kahane et al. 1984).

Line ratios, corrected for beam size and efficiency, are presented in Table 2. When correcting for beam size we require an estimate of the source size θ_s. From Imanishi et al. (2004), one can deduce an upper limit to the HCN 1–0 source size of 2″. We adopt this as θ_s for our calculations, assuming that all high-density tracer emission is emerging from the same region. Errors

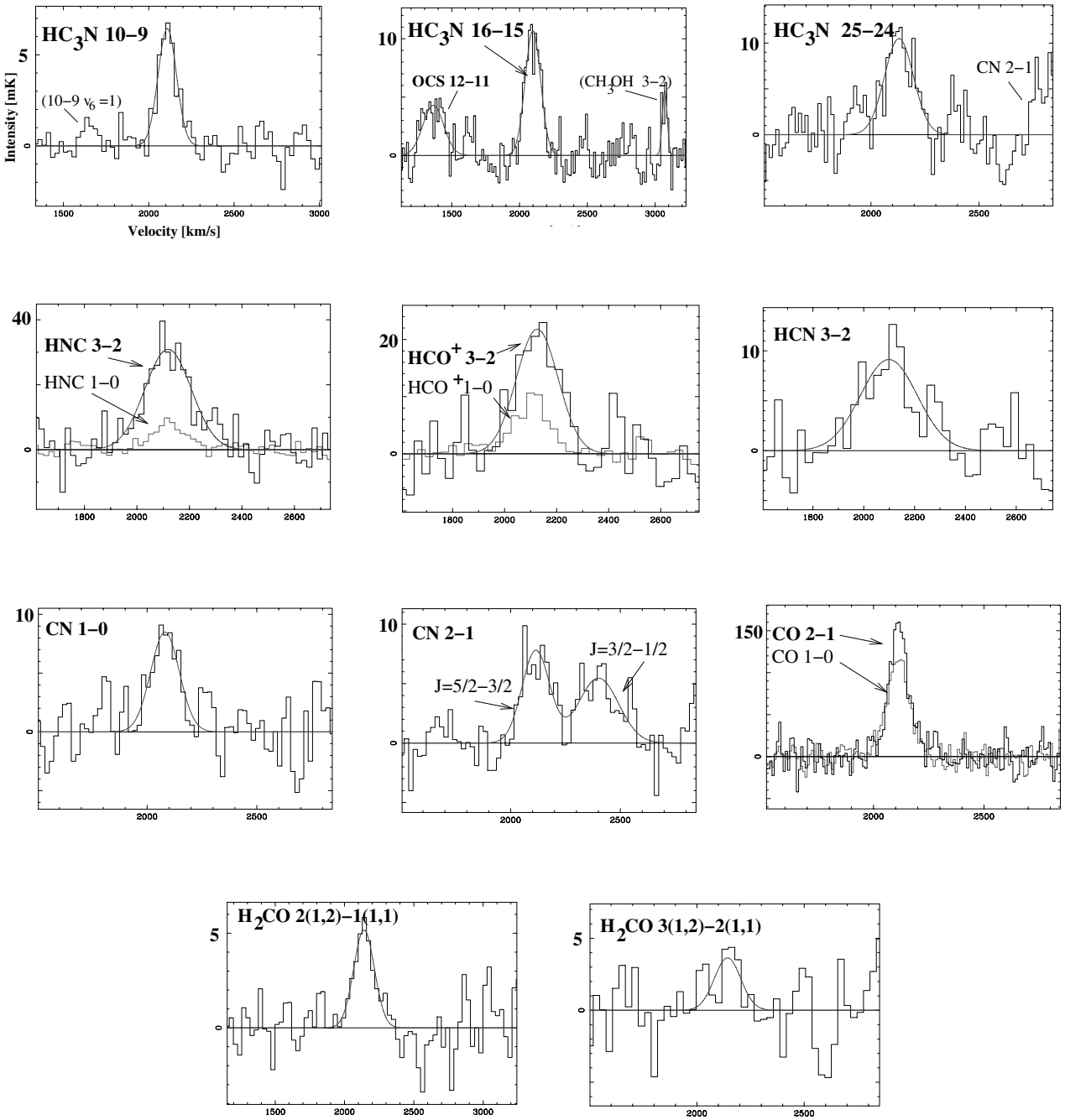

Fig. 1. Spectra of detected species towards NGC 4418 (α: 12:26:54.63, δ: -00:52:39.6) (J2000). Note that the intensity scale is T_A^* in mK and that the line intensities shown here are not corrected for beam size. *Top three panels*: velocity resolution is 15 km s^{-1}. *Left*: HC_3N 10–9 (position for 10–9 v_6 = 1–0 rotational-vibrational transition indicated). *Centre*: HC_3N 16–15 – somewhat blended with para-H_2CO (see text). Tentative line emission from OCS 12–11 towards the band edge (position of CH_3OH 3–2 indicated in spectrum). *Right*: HC_3N 25–24 (at the edge of the band the beginning of the CN 2–1 line (CN line intensity cannot be trusted). *Second row of panels*: velocity resolution is 30 km s^{-1}. *Left*: HNC 3–2 and 1–0, *centre*: HCO^+ 3–2 and 1–0, *right*: HCN 3–2. *Third row of panels*: *left*: CN 2–1 (note the two spin groups), *centre*: CN 1–0, *right*: CO 1–0 and 2–1. *Last row of two panels*: *left*: ortho H_2CO 2–1, *right*: ortho H_2CO 3–2.

in line ratios are generally 20% including rms and calibration errors, but not including source-size errors.

We do not have our own HCN 1–0 spectrum, but used the interferometric line ratio between HCN and HCO^+ 1–0 measured by Imanishi et al. (2004) to scale our observed HCO^+ 1–0 line into HCN 1–0. This rests upon the assumption that the interferometric line ratio is also correct for the single dish and that the interferometer does not miss extended HCO^+ 1–0 flux. We get an HCN 3–2/1–0 line ratio of 0.15. If we instead use the HCN 1–0 line flux directly and translate it into a 30 m observed line intensity, we get a line ratio of 0.3. We therefore adopt the line ratio of 0.22 ± 0.08 allowing for the uncertainties.

The integrated CN 2–1/1–0 line ratio should include all spingroups for 1–0 and 2–1. We only have the brightest of the two main 1–0 spingroups in our beam since the other spingroup occurs +800 km s^{-1} away from the main. Integrated intensity ratio is 0.56 (which is then too high due to the missing CN 1–0 spingroup) and the peak-to-peak is 0.31.

Table 2. Observed line ratios[a].

Species	Transitions	Line ratio
CO	2–1/1–0	0.43
HCO^+	3–2/1–0	0.42
HNC	3–2/1–0	0.75
HCN	3–2/1–0	0.22[b]
CN	2–1/1–0	0.31–0.56[c]
H_2CO	3(1, 2)–2(1, 1)/2(1, 2)–1(1, 1)	0.31
HC_3N	16–15/10–9	0.91[d]
HC_3N	25–24/10–9	0.47

[a] If θ_s is the Gaussian source size (assumed to be 2″ (see Sect. 2.1)), and θ_b is the beam size for the line, the ratio of integrated intensities for transition X and Y, corrected for beam and source-size, is assumed to scale according to $R = \frac{\int T^*_{mb}(X)dV\,(\theta_b^2(X)+\theta_s^2)}{\int T^*_{mb}(Y)dV\,(\theta_b^2(Y)+\theta_s^2)}$. Errors in line ratios are ≈20% including rms and calibration errors. [b] We used the interferometric line ratio between HCN and HCO^+ 1–0 measured by Imanishi et al. (2004) to scale our observed HCO^+ 1–0 line into an expected HCN 1–0 intensity (see Sect. 2.1). [c] Integrated intensity ratio is 0.56 (too high due to the missing CN 1–0 emission) and the peak-to-peak is 0.31 (see Sect. 2.1). [d] The line ratio is somewhat uncertain due to para-H_2CO contamination (see Sect. 2.1).

2.2. Radiative transport modelling

We used the online mean escape probability code RADEX (van der Tak et al. 2007) for radiative transport modelling of the observed molecular line ratios. The online version of RADEX assumes spherical cloud geometry. We assume that all line emission is emerging from the same gas. This is, of course, unlikely to be true, but will give a first handle on physical conditions and relative column densities.

RADEX models the average condition for a single cloud type. Here, the emission has been modelled as emerging from one structure of linewidth 150 km s^{-1}, dealing with the global line emission at once. A more realistic approach is to assume an ensemble of individual clouds with a filling factor. Furthermore, multiple cloud types and/or gradients within clouds should also be considered in a more advanced model, including issues on self-gravitation, alternative excitation and dynamics. This will be presented in Paper II, where we will also investigate the radiative excitation further. The aim of the simple approach here is to look at average relative abundances, and physical conditions indicated by the line ratios.

2.2.1. HCN, HCO^+, H_2CO and CN

The dust temperature of NGC 4418 is estimated to be high, T_d = 85 K, and emerging from a compact nuclear structure of diameter ≈70 pc (Evans et al. 2003). The dense molecular gas also appears to be spatially compact with number densities exceeding 10^4 cm^{-3} and the gas temperature should begin to approach that of the dust. The source size of the gas distribution is, however, still unknown preventing us from deducing an exact temperature of the gas. We thus generally assumed that the gas is also warm and have varied the gas kinetic temperature from T_k = 50 to 150 K in our RADEX models. We varied the gas densities n within the range 10^4–10^6 cm^{-3}. Lower densities should not result in significant line emission from any of the observed high-density tracer species, unless affected by radiative excitation (see below). Higher densities are unlikely due to the moderate excitation.

We searched for a solution that would both accomodate the greater HCN 1–0 luminosity than that of HCO^+ 1–0 (Imanishi et al. 2004) and the reverse situation for the 3–2 line, and at the same time would fit the low excitation of HCN (and the higher excitation of HCO^+). Solutions within the constraints given above could be found for a density range of $n = 5\times10^4$–10^5 cm^{-3}. Higher densities are not allowed since HCO^+ becomes thermalized. Lower densities give too low excitation even when the temperatures are allowed to exceed 150 K. The column density ratio between HCN/HCO^+ varies between 3 and 5 for the whole range of solutions. For $n = 5\times10^4$ cm^{-3}, the best fit is found for a temperature of 150 K and for $n = 1\times10^5$ for T_k = 80 K.

Ortho-H_2CO is also moderately excited, and the 3–2/2–1 line ratio agrees reasonably well with the above physical conditions, even if temperatures exceeding 80 K and 150 K, respectively, would give a better fit. The column density ratio between H_2CO/HCO^+ ranges between 1 and 3 for all solutions.

Online RADEX currently contains no datafiles for handling CN, but a rough comparison to CS can be made and RADEX run for CS with the above model parameters, which suggests that the CN line emission may also be fitted to the above conditions. CN appears to be, on average, equally abundant as HCO^+.

The ^{12}CO 2–1/1–0 line ratio is low (Table 2), requires densities of $n \lesssim 10^3$ cm^{-3}, and may not be fitted to the above model. This is due to the ^{12}CO emission emerging from a low-density nuclear component, or else the notion of a 2″ source size is not applicable for the lower transition ^{12}CO emission. The OVRO observations by Dale et al. (2005) of the CO emission show an unresolved structure in their 5″ beam. However, they recover only 35% of the flux seen on larger scales by, e.g., Young et al. (1995) and 70% of the flux seen by the 30 m CO 1–0 beam. The actual CO source size is therefore likely to be larger than the upper limit found for HCN by Imanishi et al. Yao et al. (2003) find a CO 3–2/1–0 line ratio of approximately 0.86, for a beam of about 14 arcsec. Due to the uncertainties, we do not use the CO line ratio in the model fits for the central gas.

2.2.2. HNC and HC_3N

The HC_3N and HNC line luminosities are surprisingly high and more excited than the other high density species. This points to the possibility either that HNC and HC_3N are affected by radiative excitation or that they are emerging from a denser and/or warmer cloud component than the other species.

Collisional excitation:

If we adhere to the same constraints on conditions and search in the same range as in Sect. 2.2.1., we find that the HC_3N J = 10–9 and 16–15 lines can be fitted to a component of density $n = 2\times10^5$ cm^{-3} and temperature T_k = 80 K. In this context, the HC_3N column density is high, similar to the HCN abundance. The observed 25–24 line is, however, too bright to be fitted to this model. More than 90% of the 25–24 line would have to be emerging from another component with a density $n > 10^6$ cm^{-3} to produce a luminous 25–24 line. Such a gas component would also contaminate the other high-density gas tracer lines, where the low excitation does not leave much room for such a very dense gas phase. The filling factor of a $n = 10^6$ cm^{-3} gas component would also have to be low.

A collisional excitation of HNC would require densities of $n \gtrsim 5\times10^5$ cm^{-3} for the given temperature range, which in the context of a one-component model is not an allowed density range for the HCN, HCO^+, and H_2CO line ratios.

Radiative excitation:
Pumping of HNC by 21.5 μm radiation via the degenerate bending mode has been discussed by Aalto et al. (2007) as a possibility for explaining the high HNC/HCN 3–2 line ratio in NGC 4418, Arp 220, and Mrk 231. For HNC, a mid-infrared background with a brightness temperature of 50 K will start to successfully compete with collisions at gas densities of $n < 10^4$ cm^{-3}. Thus, significant contribution to the line emission may then originate from a gas phase of lower density than the critical density for the species.

HC_3N may also be pumped via a number of infrared bending transitions, e.g. (Wyrowski et al. 1999):

- Bending mode v_5 = 1–0 at 663 cm^{-1} (956 K) with A_{ul} = 2.2 s^{-1}, 15 μm (HCC bend)
- Bending mode v_6 = 1–0 at 498 cm^{-1} (718 K) with A_{ul} = 0.15 s^{-1}, 20 μm (CCN bend)
- Bending mode v_7 = 1–0 at 223 cm^{-1} (321 K) with A_{ul} = 6×10^{-4} s^{-1}, 45 μm (CCC bend)

In Fig. 1 we indicate the position of the 10–9 v_6 = 1–0 rotational-vibrational line as a 2σ detection, but more observations are needed to show whether this feature is real or just a baseline uncertainty. Rotational-vibrational transitions of HC_3N have been observed in the Galaxy towards hot cores (e.g. Wyrowski et al. 1999).

Column density comparison:
If HC_3N line emission is affected by radiative excitation, it may have a larger filling factor than the line emission from unaffected molecular lines, such as HCN. Column density estimates done under the assumption of collisional excitation from the same gas may therefore overestimate the relative HC_3N abundance.

For NGC 4418 this may largely be related to the mass fraction of lower-density gas, in relation to the high-density gas fraction. We expect the HC_3N abundances to be lower in the low-density gas phase since this phase should be more vulnerable to photodestruction. Furthermore, the mass fraction of low-density gas in galactic nuclei is often found to be significantly lower than that of the high-density gas mass fraction, even if the lower-density gas has a higher filling factor (e.g. Aalto et al. 1994, 1995). We therefore estimate the errors in the abundance estimate due to potential radiative excitation as rather small: within factors of a few. Errors due to insufficient data and model over-simplification may be significantly greater. Observations of more HC_3N transitions will help establish to what degree radiative excitation may affect the line intensities of the rotational transitions.

3. Discussion

3.1. Interpreting the HC_3N line emission

The relative HC_3N 10–9 line emission in NGC 4418 is one of the highest measured in a galaxy on these scales comparable to what is found for Arp 220 (Aalto et al. 2002; Martin-Pintado et al., in preparation). The implied HC_3N column densities rival those of HCN, suggesting unusually large abundances. How can we understand the luminous HC_3N line emission? Below we list three scenarios and their expected impact on HC_3N abundances:

- Warm dense gas: Rodriguez-Franco et al. (1998) find high HC_3N/CN abundance ratios in hot cores (warm, star-forming, dense gas) which they attribute to very large HC_3N abundances (X[HC_3N] $\approx$ 10^{-8}) caused largely by evaporation of icy grain mantles and low destuctive cosmic-ray and UV fluxes. HC_3N can also be formed via the neutral-neutral reaction: C_2H_2 + CN $\rightarrow$ HC_3N + H (e.g. Meier & Turner 2005).

- PDRs: HC_3N is easily destroyed by UV photons (destruction rate 5.5×10^{-9} s^{-1}) and very rapidly so via reactions with the ions C^+ and He^+ (Prasad & Huntress 1980; Turner et al. 1998). Thus, we do not expect luminous HC_3N line emission from PDRs, since it would quickly become destroyed by photodissociation or by reaction with C^+. This is also observed by Rodriguez-Franco and collaborators towards PDRs in the Orion complex.

- XDRs: X-rays can penetrate large columns of gas and are therefore not as good as UV photons at dissociating molecules. There are UV photons in an XDR, but mostly in the form of relatively weak, secondary far-UV photons. Their impact on HC_3N destruction is very likely less than in a PDR. An XDR is characterised (among other things) by high abundances of C^+ and, in particular, He^+ that coexist with neutrals like CO and C. Both C^+ and He^+ are sources for HC_3N destruction. The He^+ abundances in XDRs can be five times higher than those in PDRs according to to XDR/PDR models (Meijerink & Spaans 2005). In the absence of icy-mantle grain processing and of important ion-neutral fomation mechanisms, the neutral-neutral formation mechanism indicated above will be too slow to keep up with the destruction proceeses.

HC_3N abundances are low in PDRs and we also expect them to be so in XDRs – although no direct obervations exist, and detailed modelling is required to determine abundances. From Galactic work, it is well known that the molecule thrives in hot cores and in cold dark clouds. It has been observed at high resolution in the nearby galaxy IC 342 by Meier & Turner (2005), where they find the 10–9 emission to be strongly correlated with 3 mm continuum emission interpreted as sites of ongoing star formation.

3.2. The HCN/HCO^+ 1–0 line ratio and XDRs

HCO^+ is proposed by e.g. Kohno et al. (2001) to be a tracer of the fraction of the dense gas that is involved in star formation. They compared the HCN/HCO^+ 1–0 line ratio in a selection of Seyfert and starburst galaxies and find that the relative HCO^+ 1–0 luminosity is significantly higher in starbursts. According to models by Maloney et al. (1996), a deficiency in HCO^+ is expected near a hard X-ray source – in an X-ray dominated region (XDR) – resulting in an elevated observed HCN/HCO^+ line intensity ratio. Interestingly, elevated HCN/HCO^+ 1–0 line ratios have been found in ULIRGs by Gracia-Carpio (2006), and in general the line ratio appears to correlate with FIR luminosity. The authors attribute this to the presence of an AGN where the X-rays affect the chemistry to impact the HCN/HCO^+ abundance ratio.

Abundances cannot be directly deduced from the HCN/HCO^+ 1–0 line ratio, even if the emission is indeed emerging from the same gas. Excitation effects must be taken into account. Imanishi et al. (2004) report an HCN/HCO^+ 1–0 line ratio of 1.8 for NGC 4418, suggesting that this supports the notion of an XDR. We observe, however, the opposite case for the 3–2 transitions and find that both the 1–0 and 3–2 line ratios

can be fitted to a rather moderate HCN/HCO^+ abundance ratio (see Sect. 2.2.1).

Furthermore, recent XDR modelling suggests that underabundant HCO^+ may not be an expected feature of an XDR. In contrast, for a wide range of conditions, Meijerink & Spaans (2005) and Meijerink et al. (2006) find the HCO^+ abundances exceeding those of HCN in the XDR. In their models, HCN is more abundant than HCO^+ at the edges of the XDR, but in these regions molecular abundances are generally low and do not contribute significantly to the total line luminosity. A discussion of this can also be found in Aalto et al. (2007).

Relatively low HCO^+ abundances may be expected in young, synchrotron-deficient starbursts, which would also result in HCN/HCO^+ 1–0 line intensity ratios exceeding unity. An alternative interpretation to an elevated HCN/HCO^+ 1–0 line ratio may therefore be that some Seyfert nuclei are surrounded by regions of very young star formation. If the starburst is young enough not to have produced a significant number of supernovae, then the relative HCO^+ 1–0 luminosity may be low compared to that of HCN 1–0.

3.3. CN and HNC

All XDR models predict high abundances of CN, a radical that is also abundant in PDRs (e.g. Rodriguez-Franco et al. 1998). For both XDRs and PDRs, the CN abundance is expected to be significantly higher (orders of magnitude) than that of HCN. For NGC 4418, CN is detected, but line emission appears to suggest abundances less than HCN.

Luminous HNC emission has been observed towards a sample of warm galaxies (e.g. Aalto et al. 2002) and overluminous HNC 3–2 in three galaxies (Aalto et al. 2007). Low HNC abundances are observed towards hot, dense cores in the Galaxy (e.g. Schilke et al. 1992), while equal HCN and HNC abundances are expected in a PDR (e.g. Aalto et al. 2002; Meijerink et al. 2006). In dense XDRs ($n \gtrsim 10^5$ cm^{-3}), Meijerink et al. (2006) predict HNC/HCN abundance ratios of two. Mid-IR pumping may boost the HNC luminosity relative to the HCN luminosity. For NGC 4418, the HNC emission may emerge either from a PDR component (and affected by radiative excitation) or from a deeply embedded, dense XDR.

3.4. NGC 4418: buried AGN or nascent starburst?

We find a rich molecular chemistry in NGC 4418 and luminous HC_3N line emission, which in our Galaxy is associated with warm, dense starforming cores. In this context, the elevated HCN/HCO^+ 1–0 line ratio found by Imanishi et al. (2004) may instead indicate young star formation. As discussed in Sect. 3.2, we advise caution in using the HCN/HCO^+ 1–0 line ratio as a diagnostic tool for XDR activity, since its interpretation is ambiguous. It is clear that further XDR modelling is required, including a continued discussion of the HCN/HCO^+ line emission ratio, as well as modelling HC_3N abundances in XDRs.

For NGC 4418, we tentatively suggest that the line emission can be fitted to a combination of a warm, dense gas component not strongly affected by UV or cosmic rays (hot-core like chemistry) supplying abundant HC_3N and HCN with an additional PDR component (providing CN, HCO^+ and HNC line emission). This scenario is consistent with the suggestion by Roussel et al. that the high q-factor is due to a young starburst. They also propose that NGC 4418 is probably in a somewhat later evolutionary stage than other high-q objects, since it does contain a synchrotron source and contains both a nascent starburst and a more evolved component.

3.4.1. Future observational tests

Even though we suggest a starburst explanation for the observed line ratios, a deeply embedded AGN, surrounded by star formation, cannot be excluded. Without high-resolution information, we cannot tell whether the HC_3N line emission is emerging from farther out than, for instance, the HCN or HCO^+ line emission. In general, observations at higher resolution will help resolve the dispute about XDRs vs. star formation. Below we list other observational tests of the molecular ISM:

- Alternative and more unambigious XDR diagnostics are provided by highly excited ($J > 10$) rotational lines of ^{12}CO (Meijerink et al. 2006; Aalto et al. 2007). XDRs produce very warm ^{12}CO compared to, for example, PDRs. Other lines that can help distinguish between XDRs, PDRs, and young star formation include HOC^+, NO, CO^+, and CS (e.g. Meijerink et al. 2007).
- Observing higher J lines of all detected molecular species allows for more detailed modelling of the physical conditions in the gas. For HC_3N, these observations – as well as a search for the rotational-vibrational lines – should reveal a possible pumping situation. This is also important for the HNC line emission.
- High-resolution observations of molecular lines help determine from where the line emission is emerging. The upcoming ALMA (Atacama Large Millimeter Array) observatory will provide unprecedented spatial resolution that will allow cloud-scale observations of many of the luminous galaxies. Dynamical studies of the nuclear gas will enable measurements of enclosed masses and searches for molecular outflows.

4. Conclusions

1. We have, with the IRAM 30m telescope, searched for line emission from high-density tracer molcecules towards the luminous, deeply obscured galaxy NGC 4418. We have detected line emission from HNC, HCN, HCO+ J = 1–0 and 3–2, CN 1–0 and 2–1, HC_3N 10–9, 16–15, 25–24, ortho-H_2CO 3–2, 2–1 (and tentatively OCS 12 –11). All species have low excitation with the exception of HNC and HC_3N which are more highly excited.
2. The HC_3N line emission is unusually luminous, in particular the 10–9 line with an intensity similar to that of CN 1–0. This suggests large abundances of HC_3N, a molecule often associated with young star formation.
3. We find overluminous HNC 3–2 emission, where the HNC luminosity is a factor of 2.3 times that of HCN 3–2. This has led us to propose that HNC may be pumped by 20 μm IR continuum (Aalto et al. 2007). The high excitation of HC_3N is also consistent with radiative excitation.
4. We find an HCN/HCO^+ 3–2 ratio of about 0.5. Imanishi et al. (2004) report the opposite for the 1–0 ratio. The HCN, HCO^+, H_2CO line ratios can be fitted to a single cloud component with T_k = 80−150 K, gas densities of 5×10^4−1×10^5 cm^{-3}, and an HCN/HCO^+ abundance ratio of ≈3.
5. The HCN/HCO^+ 1–0 line ratio has previously been suggested to indicate the presence of an XDR associated with an AGN. We find, however, that the molecular line ratios are

also consistent with a young starburst, in particular the luminous HC_3N line emission. We advise caution in using elevated HCN/HCO^+ line ratios as XDR indicators, since the interpretation is not unique.

Acknowledgements. Many thanks to the IRAM staff for friendly help and support. We are grateful to M. Wiedner for discussions and comments on the manuscript. We thank the anonymous referee for useful comments that helped improve the manuscript.

References

Aalto, S., Polatidis, A. G., Hüttemeister, S., & Curran, S. J. 2002, A&A, 381, 783
Aalto, S., Spaans, M., Wiedner, M. C., & Hüttemeister, S. 2007, A&A, 464, 193
Cagnoni, I, della Ceca, R., & Maccacaro, T. 1998, ApJ, 493, 54
Dale, D. A., Sheth, K., Helou, G., Regan, M. W., & Hüttemeister, S. 2005, AJ, 129, 2197
Evans, A. S., Becklin, E. E., Scoville, N. Z., et al. 2003, AJ, 125, 2341
Graciá-Carpio, J., García-Burillo, S., Planesas, P., & Colina, L. 2006, ApJ, 640, 135
Imanishi, M., Nakanishi, K., Kuno, N., & Kohno, K. 2004, AJ, 128, 2037
Irvine, W. M., Goldsmith, P. F., & Hjalmarson, Å 1987, in Interstellar Processes, ed. D. J. Hollenback, & H. A. Jr Thronson (Dordrecht: D. Reidel Publishers Co.), 561
Kahane, C., Lucas, R., Frerking, M. A., Langer, W. D., & Encrenaz, P. 1984, A&A, 137, 211
Kohno, K., Matsushita, S., Vila-Vilaro, B., et al. 2001, in The Central Kiloparsec of Starbursts and AGN: The La Palma Connection, ed. Knapen, Beckman, Shlosman, & Mahoney, ASP Conf. Ser., 249, 672
Maloney, P. R., Hollenbach, D. J., & Tielens, A. G. G. M. 1996, ApJ, 466, 561
Meier, D. S., & Turner, J. L. 2005, ApJ, 618, 259
Meijerink, R., Spaans, M., & Israel, F. P. 2006, ApJ, 650, L103
Meijerink, R., Spaans, M., & Israel, F. P. 2007, A&A, 461, 793
Prasad, S. S., & Huntress, W. T. 1980, ApJ, 239, 151
Rodriguez-Franco, A., Martin-Pintado, J., & Fuente, A. 1998, A&A, 329, 1097
Roussel, H., Helou, G., Beck, R., et al. 2003, ApJ, 593, 733
Schilke, P., Walmsley, C. M., Pineau de Forêts, G., et al. 1992, A&A 256, 595
Sanders, D. B., & Mirabel, I. F. 1996, ARA&A, 34, 749
Spoon, H. W. W., Keane, J. V., Tielens, A. G. G. M., Lutz, D., & Moorwood, A. F. M. 2001, A&A, 365, 353
Turner, B. E., Lee, H.-H., & Herbst, E. 1998, ApJS, 115, 91
Van der Tak, F. F. S., Black, J. H., Schöier, F. L., Jansen, D. J., & van Dishoeck, E. F. 2007, A&A 468, 627
Wyrowski, F., Schilke, P., & Walmsley, C. M. 1999, A&A, 341, 882
Yao, L., Seaquist, E. R., Kuno, N., & Dunne, L. 2003, ApJ, 588, 771
Young, J. S., Xie, S., Tacconi, L., et al. 1995, ApJS, 98, 219